CHALMERS
FINITE ELEMENT CENTER

PREPRINT 2001–16

Application of stable FEM-FDTD hybrid to scattering problems

Thomas Rylander and Anders Bondeson

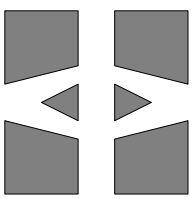

Chalmers Finite Element Center
CHALMERS UNIVERSITY OF TECHNOLOGY
Göteborg Sweden 2001

CHALMERS FINITE ELEMENT CENTER

Preprint 2001–16

Application of stable FEM-FDTD hybrid to scattering problems

Thomas Rylander and Anders Bondeson

CHALMERS

Chalmers Finite Element Center
Chalmers University of Technology
SE–412 96 Göteborg Sweden
Göteborg, September 2001

Application of stable FEM-FDTD hybrid to scattering problems
Thomas Rylander and Anders Bondeson
NO 2001–16
ISSN 1404–4382

Chalmers Finite Element Center
Chalmers University of Technology
SE–412 96 Göteborg
Sweden
Telephone: +46 (0)31 772 1000
Fax: +46 (0)31 772 3595
www.phi.chalmers.se

Printed in Sweden
Chalmers University of Technology
Göteborg, Sweden 2001

APPLICATION OF STABLE FEM-FDTD HYBRID TO SCATTERING PROBLEMS

THOMAS RYLANDER AND ANDERS BONDESON

Abstract. A recently developed, stable FEM-FDTD hybrid, that eliminates the staircase approximation of complex geometries, is tested by convergence studies for radar cross sections. For a conducting sphere, 1 dB accuracy in all directions is obtained with 9 cells per wavelength whereas the NASA almond requires a higher resolution of about 15 cells per wavelength. For scatterers with a smooth boundary, the results converge quadratically with the mesh size, but for a horizontally polarized wave incident on the NASA almond, the order of convergence is lower because of singular fields at the tip.

1. Introduction

The Finite-Difference Time-Domain (FDTD) scheme [1, 2] is very popular for electromagnetics modeling because of its simplicity and efficiency. One drawback of the FDTD is the staircase approximation of oblique boundaries, which often gives poor accuracy. The Finite Element Method (FEM) [3] allows good approximations of complex boundaries, and with edge elements [3, 4] it performs well for Maxwell's equations. However, FEM requires more memory and has a higher operation count than the FDTD. An obvious remedy is a hybrid that applies FDTD in large volumes, combined with FEM near complex boundaries. Previously attempted hybrids of this type [5, 6] suffer from instabilities known as late time growth.

We have recently constructed a FEM-FDTD hybrid [7], that is completely stable for time steps up to the Courant limit of the FDTD. It is also conservative, preserves the reciprocity of Maxwell's equations and introduces only small reflection from the interface between structured and unstructured grids [7]. In this article, we show its performance in two scattering problems, a perfect electric conducting (PEC) sphere and the NASA almond.

2. The method

To compute the radar cross section (RCS) using the hybrid method, we place the scatterer in a hexahedral simulation box. A thin layer of unstructured tetrahedral grid around the scatterer is connected to the structured FDTD grid via a single layer of pyramids. On the tetrahedrons and pyramids, the electric field is expanded in edge elements [3, 8]. The

Key words and phrases. Electromagnetic scattering, Hybrid Method, Convergence, Finite Element Method, Finite-Difference Time-Domain.

The authors are with the Department of Electromagnetics, Chalmers University of Technology, Göteborg, Sweden.

hybrid method [7] is based on the fact that the FDTD follows from FEM, using hexahedral edge elements and trapezoidal integration. The trapezoidal integration leads to "lumping" of both the "mass" matrix $\mathbf{M}$, representing $\epsilon\vec{E}$, and the "stiffness" matrix $\mathbf{S}$, representing $\nabla \times \mu^{-1}\nabla \times \vec{E}$. Thus, the hybrid method is constructed by applying FEM concepts everywhere, and it reduces to the FDTD on the hexahedral grid, where we use trapezoidal integration.

The resulting mass and stiffness matrices are symmetric everywhere, even at the FEM-FDTD interface. This is the essential difference of our approach compared to earlier, unstable hybrids [5, 6]. The symmetric matrices guarantee reciprocity and make it possible to achieve stability. With an unconditionally stable, implicit (but non-dissipative) time-stepping [9] in the FEM region, the scheme remains stable for time-steps up to the maximum for the FDTD, $h/\sqrt{3}c$, where h is the cell size. In the computations reported here, the implicitness parameter θ on the FEM grid is always set to the minimum value $\theta = 1/4$ [7] that guarantees stability for any time-step, and the maximum time-step of the FDTD is used. In the FEM region, a sparse matrix must be inverted for each time step. This is done efficiently by the conjugate gradient method with a zero-fill-in ILU-preconditioner. Nine iterations per time step typically give an error of order 10^{-6}.

An incident plane wave $E_{inc}(t) = E_0 \exp[-(t-t_0)^2/d_0^2] \sin[\omega_0(t-t_0)]$ is imposed at a Huygen's surface [2]. The radiation field is obtained from the scattered field outside the Huygen's surface by a near-to-far-field (NTF) transformation [2]. We apply an NTF transformation using third order Lagrange interpolation and four point Gauss quadrature. The transformation converges with an $O(h^4)$ error and gives a maximum error of 0.05 % when $\lambda/h = 18$. The scattered wave is absorbed at the outer boundary by a "sponge layer" [10].

3. Scattering from PEC sphere

The code was validated against analytic results for a PEC sphere. The bistatic RCS for a sphere of radius 1 m was computed on three different meshes with FDTD cell size $h = n/15\sqrt{3}$ m for $n = 9$, 6 and 4. The wavelength was $\lambda = 4.16$ m and the time constants $t_0 = 1.73 \cdot 10^{-8}$ s, $d_0 = 6.00 \cdot 10^{-9}$ s. The relative error $e(h) = ||\sigma_n - \sigma_a||_2 / ||\sigma_a||_2$ is shown in Fig. 1. Here $||\cdot||_2 = [\int_\Omega (\cdot)^2 d\Omega]^{1/2}$ and σ_n and σ_a are the numerically computed and analytic bistatic RCS. A least square fit to the model $e(h) = ch^\alpha$ gives $\alpha \simeq 2.02$. This confirms that the FEM-FDTD hybrid method converges towards the exact solution with an $O(h^2)$ error. Extrapolation indicates that a root mean square accuracy of 1 dB is obtained with 7.2 cells per wavelength. 1 dB accuracy in all directions requires 9 cells per wavelength.

One potential problem for the hybrid method is scattering at the FEM-FDTD interface. To investigate this, we replaced the interior of the sphere by vacuum, discretized by tetrahedrons. For 12 cells per wavelength, the computed σ of this grid was at least 35 dB below that of the conducting sphere in all directions.

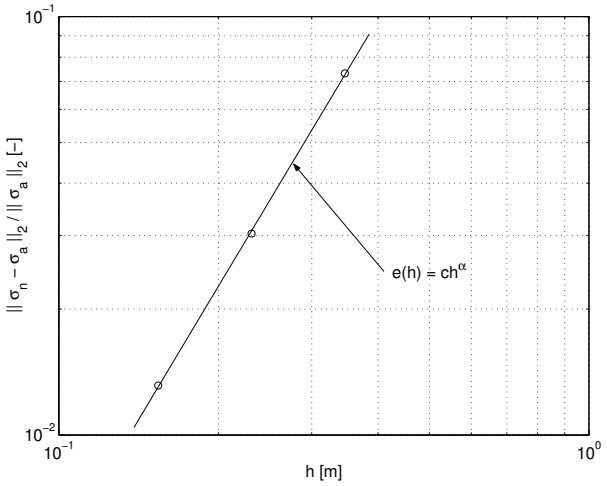

FIGURE 1. Relative error in the bistatic RCS for a PEC sphere : circles - computed results, line - fit for extrapolation.

4. Scattering from the NASA almond

We also calculated the monostatic RCS of the NASA almond [11, 12, 13] when the wavelength equals the length of the almond, $\lambda = 0.2524$ m.

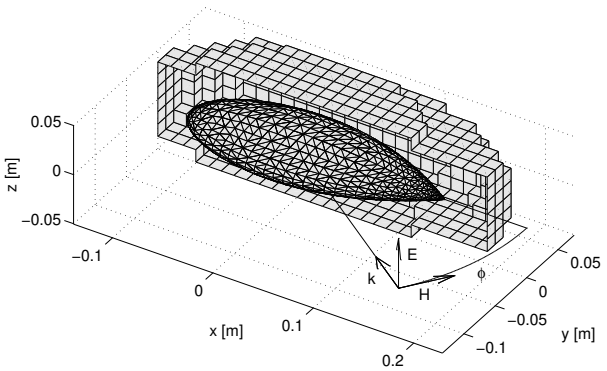

FIGURE 2. The discretized almond and an incident plane wave with vertical polarization.

Here, we chose $t_0 = 3.31 \cdot 10^{-8}$ s, $d_0 = 1.15 \cdot 10^{-8}$ s, and the sponge layer was 0.101 m thick. The unstructured grid, shown in Fig. 2, has increased resolution at the tip of the almond. For the convergence study, we rescaled the mesh size uniformly.

Following the notation in [2], the complex scattering amplitudes N_θ, N_ϕ, L_θ and L_ϕ were calculated for incidence angles $\phi_m = m\pi/16$, $m = 0, 1, \ldots, 16$ on 6 different meshes with FDTD cell size $h = \lambda/5n$, where we took $n = 3$, 4, 5, 6, 8 and 12. The RCS for horizontal and vertical polarization computed on the six different grids are shown in Fig. 3.

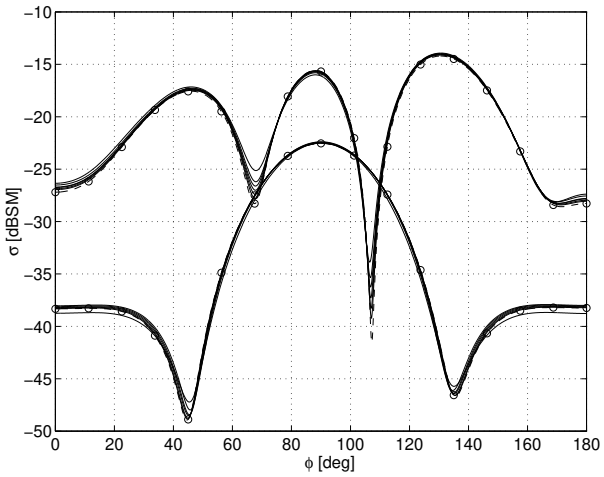

FIGURE 3. RCS for horizontal and vertical polarization on the six different grids, shown by upper and lower sets of curves respectively. The extrapolated results are shown as circles joined by dashed curves.

Even though the hybrid method is a second order scheme, quadratic convergence cannot be expected for the NASA almond because of singular fields at the tip [14]. We anticipate that the scattering amplitudes converge, to lowest order, as $\tilde{L} = L_0 + L_\alpha h^\alpha$ for some power α. To find the order of convergence for horizontal polarization, we minimized the mean square error $e = [\Sigma_{\phi_m}(|Z_0(N_\phi - \tilde{N}_\phi)|^2 + |L_\theta - \tilde{L}_\theta|^2)]^{1/2}$ with respect to α (N_ϕ and L_θ denote numerically computed amplitudes and $\tilde{N}_\phi$ and $\tilde{L}_\theta$ denote the fit). This procedure allows the order of convergence to be fairly accurately determined, despite some uneven variations with element size caused by the unstructured grid. We found the order of convergence to be 2 for vertical polarization and about 1.2 for horizontal polarization. Finally, we fitted the functions $\tilde{L} = L_0 + L_2 h^2$, for vertical polarization, and $\tilde{L} = L_0 + L_1 h^{1.2} + L_2 h^2$, for horizontal polarization, to extrapolate to the result L_0 for zero mesh size.

Figure 4 shows the computed RCS and the fit versus h for horizontal polarization and certain angles of incidence. Figure 5 shows the estimated error $\Delta\sigma[\text{dB}] = 10\log(\sigma/\sigma_0)$ versus ϕ, for the coarsest ($\lambda/h = 15$) and finest ($\lambda/h = 60$) grids and both polarizations. The relative errors are the largest near the minima of the RCS. For horizontal polarization and $\lambda/h = 60$, the relative error peaks at about 2.5 dB around $\phi = 107°$. However, for most ϕ the estimated error is below 0.25 dB when $\lambda/h = 60$. For vertical polarization and $\lambda/h = 60$, the estimated error is at most 0.3 dB. For both polarizations, $\lambda/h = 15$ gives an accuracy better than 1 dB for at least 90% of the azimuth angles.

Previous results for the NASA almond have been given by Woo et al. for the FERM code [11] and Bluck and Walker for the Zeus code [12, 13], both based on the Method of Moments. For vertical polarization, the difference between our extrapolated results and those from the Zeus code is less than 1 dB for all ϕ, while the FERM results are 2-5 dB higher than the others in the interval $40° < \phi < 130°$. For the horizontal polarization,

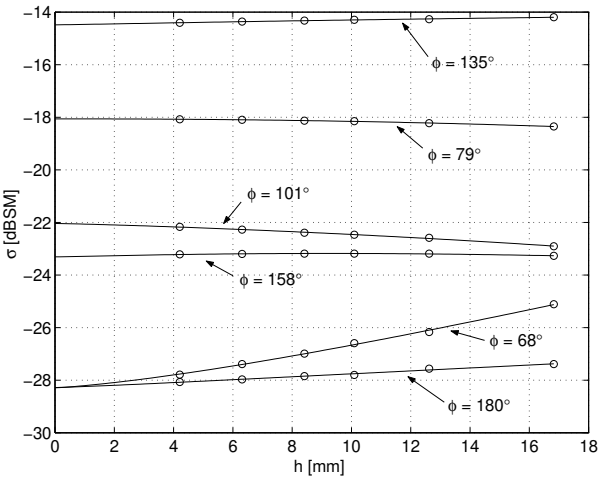

FIGURE 4. Convergence of RCS for the horizontal polarization with respect to h for different angles of incidence: circles - computed results, lines - fit for extrapolation.

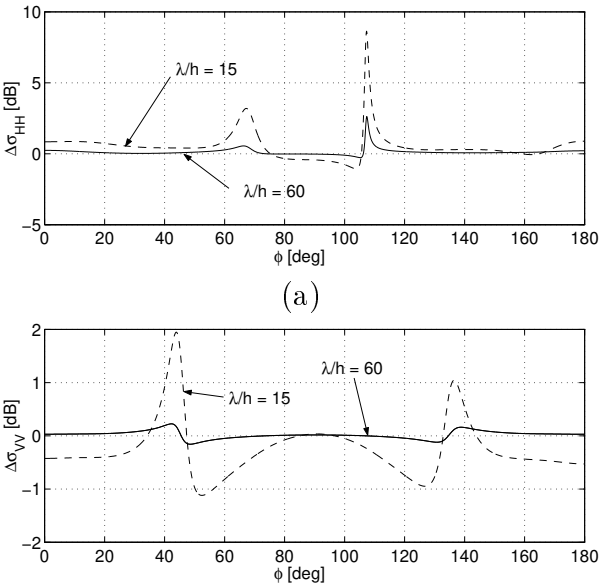

FIGURE 5. Error in RCS for (a) horizontal and (b) vertical polarization on the finest and coarsest grid.

the differences are larger. The results from FERM and Zeus typically differ by 2 dB, and the FEM-FDTD hybrid method stays roughly in between the FERM and Zeus results. After the careful convergence study carried out here, we would tentatively claim that our

extrapolated values have an accuracy of about ± 0.1 dB, except near the minima for the horizontal polarization.

5. Conclusions

We have applied the stable FEM-FDTD hybrid [7] to compute the RCS of a PEC sphere and the NASA almond. For the PEC sphere, the bistatic RCS converges to the analytical solution with an $O(h^2)$ error. For $ka = 1.5$, where k is the wavenumber and a the radius of the sphere, the maximum error in the bistatic RCS is 1 dB when the FDTD grid has 9 points per wavelength.

For the NASA almond, we found the order of convergence for the hybrid method to be 2 for vertical polarization and about 1.2 for horizontal polarization. The poorer convergence for horizontal polarization is caused by singular fields at the tip of the almond. The RCS computed with $\lambda/h = 15$, and the length of the almond equal to the wavelength, deviates less than 1 dB from the extrapolated results, except where the RCS has deep minima. The accuracy of the results extrapolated to zero cell size can be estimated as ± 0.1 dB except close to the minima for horizontal polarization.

The stable FEM-FDTD hybrid has many advantages. It combines the high efficiency of the FDTD with the ability of the FEM to model complex geometry. Since the number of operations per unit volume is roughly a factor 20 higher for the FEM part, the FEM region should be small, which can readily be achieved when the grid size is small. Furthermore, because the time stepping in the FEM region is unconditionally stable, fine details can be resolved without the reduction of time-step needed for explicit schemes.

Acknowledgments

This work was supported in part by grants from National Graduate School of Scientific Computing (NGSSC) and the Technical Research Foundation (TFR).

References

[1] K. S. Yee, "Numerical solution of initial boundary value problems in isotropic media," *IEEE Trans. Antennas Propagat.,* vol. AP-14, pp. 302-307, May 1966.

[2] A. Taflove, *Computational Electrodynamics: The Finite-Difference Time-Domain Method,* Norwood, MA: Artech House, 1995.

[3] J. Jin, *The Finite Element Method in Electromagnetics,* New York: Wiley, 1993.

[4] J. C. Nédélec, "Mixed finite elements in R^3," *Numer. Math.,* vol. 35, no. 3, pp. 315-341, 1980.

[5] R. B. Wu and T. Itoh, "Hybrid Finite-Difference Time-Domain Modeling of Curved Surfaces Using Tetrahedral Edge elements," *IEEE Trans. Antennas Propagat.,* vol. 45, no. 8, pp. 1302-1309, August 1997.

[6] A. Monorchio and R. Mittra, "A hybrid Finite-Element Finite-Difference Time-Domain (FE/FDTD) technique for solving complex electromagnetic problems," *IEEE Microw. Guided Wave Lett.,* vol. 8, pp. 93-95, February 1998.

[7] T. Rylander and A. Bondeson, "Stable FEM-FDTD hybrid method for Maxwell's equations," *Comput. Phys. Comm.,* vol. 125, pp. 75-82, March 2000.

[8] J. L. Coulomb, F. X. Zgainski and Y. Maréchal, "A Pyramidal Element to link Hexahedral, Prismatic and Tetrahedral Edge Finite Elements," *IEEE Trans. Magnetics,* vol. 33, no. 2, pp. 1362-1365, March 1997.

[9] J. F. Lee, R. Lee and A. Cangellaris, "Time-Domain Finite-Element Methods," *IEEE Trans. Antennas Propagat.,* vol. 45, no. 3, pp. 430-442, March 1997.

[10] P. G. Petropoulos, L. Zhao and A. C. Cangellaris, "A Reflectionless Sponge Layer Absorbing Boundary Condition for the Solution of Maxwell's Equations with High-Order Staggered Finite Difference Schemes," *J. Comput. Phys.,* vol. 139, pp. 184-208, January 1998.

[11] A. C. Woo, H. T. G. Wang, M. J. Schuh and M. L. Sanders, "Benchmark Radar Targets for the Validation of Computational Electromagnetics Programs," *IEEE Antennas Propagat. Mag.,* vol. 35, no. 1, pp. 84-89, February 1993.

[12] M. J. Bluck and S. P. Walker, "Time-Domain BIE Analysis of Large Three-Dimensional Electromagnetic Scattering Problems," *IEEE Trans. Antennas Propagat.,* vol. 45, no. 5, pp. 894-901, May 1997.

[13] M. J. Bluck and S. P. Walker, "Benchmark RCS results," http://www.me.ic.ac.uk/mechanics/CWP/CWP_benchmarks/CWP_benchmarks.html .

[14] R. de Smedt, "Electric Singularity Near the Tip of a Sharp Cone," *IEEE Trans. Antennas Propagat.,* vol. 36, no. 1, pp. 152-155, January 1988.

Chalmers Finite Element Center Preprints

2000–01 *Adaptive Finite Element Methods for the Unsteady Maxwell's Equations*
Johan Hoffman

2000–02 *A Multi-Adaptive ODE-Solver*
Anders Logg

2000–03 *Multi-Adaptive Error Control for ODEs*
Anders Logg

2000–04 *Dynamic Computational Subgrid Modeling* (Licentiate Thesis)
Johan Hoffman

2000–05 *Least-Squares Finite Element Methods for Electromagnetic Applications* (Licentiate Thesis)
Rickard Bergström

2000–06 *Discontinuous Galerkin Methods for Incompressible and Nearly Incompressible Elasticity by Nitsche's Method*
Peter Hansbo and Mats G. Larson

2000–07 *A Discountinuous Galerkin Method for the Plate Equation*
Peter Hansbo and Mats G. Larson

2000–08 *Conservation Properties for the Continuous and Discontinuous Galerkin Methods*
Mats G. Larson and A. Jonas Niklasson

2000–09 *Discontinuous Galerkin and the Crouzeix-Raviart element: Application to elasticity*
Peter Hansbo and Mats G. Larson

2000–10 *Pointwise A Posteriori Error Analysis for an Adaptive Penalty Finite Element Method for the Obstacle Problem*
Donald A. French, Stig Larson and Ricardo H. Nochetto

2000–11 *Global and Localised A Posteriori Error Analysis in the Maximum Norm for Finite Element Approximations of a Convection-Diffusion Problem*
Mats Boman

2000–12 *A Posteriori Error Analysis in the Maximum Norm for a Penalty Finite Element Method for the Time-Dependent Obstacle Problem*
Mats Boman

2000–13 *A Posteriori Error Analysis in the Maximum Norm for Finite Element Approximations of a Time-Dependent Convection-Diffusion Problem*
Mats Boman

2001–01 *A Simple Nonconforming Bilinear Element for the Elasticity Problem*
Peter Hansbo and Mats G. Larson

2001–02 *The $\mathcal{LL}^*$ Finite Element Method and Multigrid for the Magnetostatic Problem*
Rickard Bergström, Mats G. Larson, and Klas Samuelsson

2001–03 *The Fokker-Planck Operator as an Asymptotic Limit in Anisotropic Media*
Mohammad Asadzadeh

2001–04 *A Posteriori Error Estimation of Functionals in Elliptic Problems: Experiments*
Mats G. Larson and A. Jonas Niklasson

2001–05 *A Note on Energy Conservation for Hamiltonian Systems Using Continuous Time Finite Elements*
Peter Hansbo

2001–06 *Stationary Level Set Method for Modelling Sharp Interfaces in Groundwater Flow*
Nahidh Sharif and Nils-Erik Wiberg

2001–07 *Integration methods for the calculation of the magnetostatic field due to coils*
Marzia Fontana

2001–08 *Adaptive finite element computation of 3D magnetostatic problems in potential formulation*
Marzia Fontana

2001–09 *Multi-Adaptive Galerkin Methods for ODEs I: Theory & Algorithms*
Anders Logg

2001–10 *Multi-Adaptive Galerkin Methods for ODEs II: Applications*
Anders Logg

2001–11 *Energy norm a posteriori error estimation for discontinuous Galerkin methods*
Roland Becker, Peter Hansbo, and Mats G. Larson

2001–12 *Analysis of a family of discontinuous Galerkin methods for elliptic problems: the one dimensional case*
Mats G. Larson and A. Jonas Niklasson

2001–13 *Analysis of a nonsymmetric discontinuous Galerkin method for elliptic problems: stability and energy error estimates*
Mats G. Larson and A. Jonas Niklasson

2001–14 *A hybrid method for the wave equation*
Larisa Beilina, Klas Samuelsson, Krister Åhlander

2001–15 *A Finite Element Method for Domain Decomposition with Non-Matching Grids*
Roland Becker, Peter Hansbo and Rolf Stenberg

2001–16 *Application of stable FEM-FDTD hybrid to scattering problems*
Thomas Rylander and Anders Bondeson

These preprints can be obtained from

`www.phi.chalmers.se/preprints`